International Journal of Nanomedicine

Dovepress
Taylor & Francis Group

Open Access Full Text Article

ORIGINAL RESEARCH

ZnPPIX-Loaded Nanoemulsions Reprogram Immunosuppressive Macrophages in Vitro: A Potential Strategy for Glioblastoma Microenvironment Modulation

Ada Tushe[1], Elena Marinelli[2], Sara Zumerle[1], Valentina Andretto[3], Hanäé Guérin[3], Annavera Ventura[1], Olga Slukinova[2], Giulia Zampardi[1], Francesco Volpin[4], Camilla Bonaudo[5], Alessandro Della Puppa[5], Giovanna Lollo[3,6], Susanna Mandruzzato[1,2]

[1]Immunology and Molecular Oncology Unit, Veneto Institute of Oncology (IOV)—IRCCS, Padua, Italy; [2]Department of Surgery, Oncology and Gastroenterology, University of Padua, Padua, Italy; [3]Laboratoire D'Automatique, de Génie des Procédés et de Génie Pharmaceutique, LAGEPP UMR 5007, University Lyon 1, CNRS, Lyon, France; [4]Neurosurgery Department, University Hospital of Padova, Padova, Italy; [5]Neurosurgery, Department of Neurofarba, University of Florence, University Hospital of Careggi, Florence, 50134, Italy; [6]Institut Universitaire de France (IUF), Paris, France

Correspondence: Susanna Mandruzzato, Immunology and Molecular Oncology Unit, Veneto Institute of Oncology IOV—IRCCS, Via Gattamelata, n.64, Padova, 35128, Italy, Tel +390498215898, Fax +390498072854, Email susanna.mandruzzato@unipd.it

Background: Glioblastoma (GBM) is a highly malignant primary brain tumor with an overall survival of less than 15 months, despite aggressive treatment. While immunotherapy has shown success in other cancers, it has been largely ineffective in GBM, partly because of the immunosuppressive microenvironment driven by bone marrow-derived macrophages (BMDMs). This immunosuppressive milieu hinders the efficacy of both standard and immune therapies, and highlights the urgent need for novel targeted approaches. Nanomedicine offers promising solutions by enabling selective targeting of tumor-promoting cells, especially in the challenging tumor microenvironment (TME) of GBM. We previously demonstrated that the inhibition of heme-oxygenase-1 (HO-1), an enzyme central to iron metabolism, has the potential to reprogram BMDMs towards a more pro-inflammatory and anti-tumor phenotype.

Methods: Using a microfluidic-based approach, we successfully developed an oil-in-water (O/W) nanoemulsion loaded with the HO-1 inhibitor, zinc protoporphyrin IX (NE-ZnPPIX), with optimal characteristics for therapeutic application. The intrinsic fluorescence of ZnPPIX allowed the tracking of its cellular uptake. Functional assays including phenotypic marker analysis and suppression assays were performed to assess the immunomodulatory effects of NE-ZnPPIX on macrophages.

Results: Studies on cells derived from GBM patients revealed that NE-ZnPPIX could be selectively internalized by immunosuppressive myeloid cells (particularly BMDMs), malignant cells within the TME, and circulating monocytes while showing minimal uptake by lymphocytes. Our study demonstrated that encapsulated ZnPPIX, similar to free ZnPPIX, effectively reduced the immunosuppressive activity of in vitro-derived macrophages. Furthermore, NE-ZnPPIX showed superior efficacy in modulating macrophage activity by decreasing the expression of CD163, a marker associated with the pro-tumoral immunosuppressive phenotype.

Conclusion: Our findings suggest that NE-ZnPPIX may represent a novel and effective strategy for remodeling the immunosuppressive TME of GBM in combination with established immune-stimulating therapies. This approach has the potential to enhance the efficacy of immunotherapy by overcoming the tumor immune evasion mechanisms.

Keywords: nanoemulsions, tumor microenvironment, glioblastoma, zinc protoporphyrin IX, macrophages

Introduction

Immature myeloid populations and tumor-associated macrophages (TAMs) are immunosuppressive subsets frequently enriched in cancer patients. These dysfunctional cells play a key role in suppressing anti-tumor immunity and are linked to unfavorable clinical outcomes. Therefore, therapeutic targeting of these myeloid cells offers a promising approach to counteract tumor-induced immunosuppression and enhance cancer prognosis.[1] Glioblastoma multiforme (GBM) is

Received: 6 June 2025
Accepted: 27 August 2025
Published: 6 October 2025

Graphical Abstract

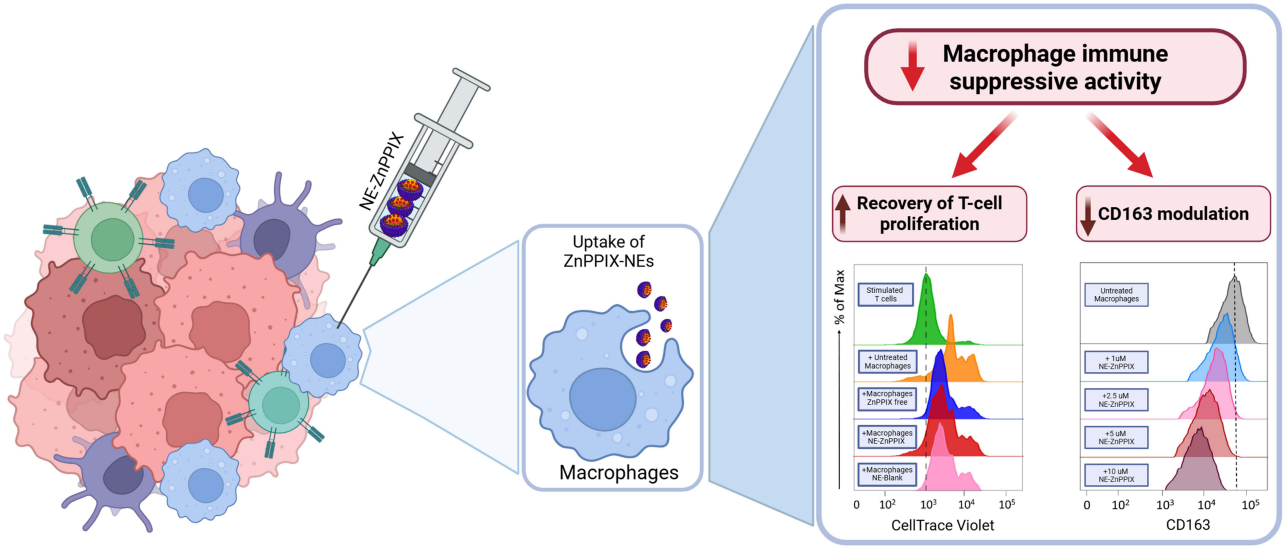

a highly aggressive primary brain tumor distinguished by a profoundly immunosuppressive tumor microenvironment (TME). A defining feature of this environment is the scarce infiltration of T lymphocytes, which, when present, often exhibit phenotypic and functional markers of exhaustion. These immune-evasive characteristics lead to the classification of GBM as an immunologically "cold" tumor, contributing to its resistance to immunotherapeutic approaches.[2,3]

Previous research, including ours, has highlighted the critical role of myeloid cells in the TME of GBM. Specifically, we demonstrated that bone marrow-derived macrophages (BMDMs) exhibit a markedly enhanced intrinsic ability to suppress immune responses compared to resident microglial cells (MG). Furthermore, BMDMs progressively infiltrate the tumor periphery to its core, where they accumulate and exert robust immunosuppressive activity.[4]

Within the TME, TAMs can be functionally reprogrammed to support tumor growth and progression. Although conventional TAM-targeted therapies have largely relied on macrophage depletion, recent studies indicate that strategies aimed at re-educating TAMs toward a pro-inflammatory and anti-tumor phenotype may offer a more effective therapeutic alternative.[5]

Targeting specific cell subsets within the TME in GBM can indeed be beneficial, but it poses several challenges due to the distinctive features of the brain and the intricate cellular and molecular composition of the TME in GBM.[6–8] It is widely recognized that such tumors have a high recurrence rate despite the aggressive standard of care regimen.[9–11] Understanding the features of the GBM, TME has significant potential for innovative approaches to cancer treatment. Immunotherapy has exhibited notable success in combating certain aggressive cancers, and has been investigated for GBM. However, the clinical outcomes of GBM are still unsatisfactory.[7,12] Therefore, there is a pressing need to discover effective therapeutics, as no FDA-approved immunotherapy is available for its treatment.[7,13] A promising avenue currently under active investigation involves overcoming the immunosuppressive microenvironment inherent in GBM, with the goal of improving patient treatment outcomes.

Recently, we demonstrated that iron metabolism and immunosuppressive activity of BMDMs, are strictly associated and controlled by the key-enzyme heme-oxygenase 1 (HO-1).[14] Our research showed that zinc protoporphyrin IX (ZnPPIX), a potent inhibitor of HO-1, relieved the immunosuppressive activity of macrophages. Therefore, in this study, we propose a nanoemulsion-based strategy for the encapsulation of ZnPPIX to overcome its pharmacokinetic limitations, including its high hydrophobicity and rapid clearance, and to promote sustained drug release. Moreover, since the target cells are macrophages, the nanosystem exploits their natural phagocytic activity, enabling preferential uptake within the immunosuppressive GBM microenvironment. The field of nanomedicine continues to transform healthcare, particularly cancer treatment. Ongoing advancements have led to the clinical approval of over 50 nanosized

formulations, with more than 80 currently in clinical trials.[15] Among its various applications, cancer nanomedicine has attracted the most attention, largely because of the success of approved formulations, such as Doxil and Abraxane. The development of tailored formulations has enabled encapsulation and delivery of various compounds that would otherwise require organic solvents or toxic excipients.[16] In this study, we developed a nanoemulsion system loaded with ZnPPIX to achieve a high entrapment efficiency of a hydrophobic drug. Our previous work demonstrated the successful incorporation of hydrophobic compounds such as tacrolimus and tofacitinib into an optimized nanoemulsion using a microfluidic-based formulation technique.[17,18] Here, we further highlight the versatility of this formulation, not only for ZnPPIX encapsulation but also for targeted delivery to immunosuppressive cells within the TME.

Materials and Methods

Patient Characteristics

Patients were enrolled from the Neurosurgery Departments of Padua University Hospital and Florence University Hospital and underwent surgical procedures. The study protocol was approved by the ethical committees of IOV-IRCCS, Padua University Hospital, and Florence University Hospital, and written informed consent was obtained from all participants prior to inclusion. Four freshly resected tumor specimens were included in the analysis, comprising three cases of GBM (glioma grade 4, IDH1 wild-type) and one case of relapsed GBM. All diagnoses were confirmed by standard histopathological and molecular analyses in accordance with the 2021 WHO classification. Tumor samples were obtained through 5-ALA fluorescence-guided surgery, with collection specifically targeting brightly fluorescent, non-necrotic core regions (as described in Pinton et al 2019), ensuring consistency and minimizing sampling-associated heterogeneity.[4] This study was conducted in full compliance with the ethical principles of the Declaration of Helsinki.

Materials

A nanoemulsion (NE) formulation was developed using a medium-chain triglyceride mixture (Miglyol® 812), acquired from CREMER OLEO GmbH & Co. KG (Hamburg, Germany), as the oil phase. Two nonionic surfactants were employed: polyoxyethylene (40) stearate (Myrj® 52), sourced from Sigma-Aldrich (St Quentin-Fallavier, France), and oleoyl polyoxyl-6 glycerides (Labrafil® M1944CS), provided by Gattefossé (Saint-Priest, France). The aqueous phase consisted of a 5 mM phosphate-buffered saline (PBS) solution at pH 7.4. Zinc(II) protoporphyrin IX (ZnPPIX), used as the active compound, was obtained from Merck KGaA (Darmstadt, Germany). All buffers and solutions were prepared using Milli-Q grade water, produced with a Milli-Q Academic purification system (Millipore, Saint Quentin, Yvelines, France).

Formulation by the Microfluidic Technique and Physicochemical Characterization of Blank and ZnPPIX-Loaded Nanoemulsions

The developed NEs consisted of a medium-chain triglyceride (MCT) oil core stabilized by a surfactant shell composed of both hydrophilic (Myrj®52) and hydrophobic (Labrafil® M1944CS) surfactants. To prepare the oil phase, MCT (1.038g) and surfactants (2.119g Myrj®52 and 0.316g of Labrafil® M1944CS), were combined and subjected to magnetic stirring at 75 rpm within a thermostatically controlled bath maintained at 65°C. 4 mL of ethanol (EtOH) were then, added to the lipid mixture and warmed until complete dissolution. The aqueous and organic phases were precisely mixed using a -NanoAssemblr® Ignite™ system (Cytiva) at a total flow rate of 10 mL/min, with a flow rate ratio of 3:1 (aqueous to organic phase). The final formulation was left overnight under a fume hood overnight (ON) to allow the evaporation of EtOH covered with aluminum paper. Once EtOH evaporation was achieved, the formulation was filtered with 0.45μm filter. To obtain drug-loaded NEs, an appropriate amount of ZnPPIX was dissolved in EtOH and then added to the organic phase. Then the same protocol indicated for the blank formulations was used for ZnPPIX-loaded NEs. The final concentration of ZnPPIX inside NE was about 0.2 mg/mL and they were stored in the fridge at 4°C. The colloidal stability of the NE was previously evaluated over a 28-day period at both 20°C and 37°C.[17] To quantify the amount of drug in the NEs, an aliquot of the formulation was diluted with methanol and analyzed using a UV-Vis-spectrophotometry (wavelength fixed at 405 nm). The ZnPPIX concentration in the sample was assessed using a calibration curve obtained using free drug dissolved in DMSO (linear range 0.25–5 μg/mL) and dilutions were made in methanol. The hydrodynamic diameters and zeta potentials of the

NEs were measured using a Malvern Zetasizer® Nano ZS (Malvern Instruments S.A., Worcestershire, UK). The Z-average diameter, representing the intensity-weighted mean hydrodynamic size, and the polydispersity index (PDI) were determined by dynamic light scattering (DLS) at 25°C with a scattering angle of 173°. Zeta potential measurements were performed via electrophoretic light scattering (ELS).Transmission electron microscopy (TEM) was performed using a Philips CM120 microscope at the Center Technologique des Microstructures" (CTμ) of the University of Lyon 1 (Villeurbanne, France). NEs were diluted at a ratio of 1:2.5 prior to image acquisition. Encapsulation efficacy of the developed NE-ZnPPIX was calculated using the following equation (1):

$$EE(\%) = \frac{\text{Concentration derived from calibration curve}}{\text{Theoretical concentration}} \text{x}100$$

Drug loading (DL) was calculated as the ratio of the mass of ZnPPIX, detected by UV-Vis-spectrophotometry in the NE, to the total mass of the NE,[17] as reported in equation (2):

$$DL(\%) = \frac{\text{Mass of ZnPPIX in NE}}{\text{Mass of NE}} \text{x}100$$

In Vitro Drug Release of ZnPPIX From NEs

The in vitro release profile of ZnPPIX from the NEs was evaluated using a dialysis method. Briefly, 2 mL of the NE suspension (0.2 mg/mL) was placed into a dialysis bag with a molecular weight cutoff of 10 kDa (Thermo Scientific) and dialyzed against phosphate-buffered saline (PBS, pH 6.0) at 37 ± 0.5 °C, under constant stirring at 75 rpm. At scheduled time intervals, an aliquot of the NEs was collected from the dialysis bag. The amount of drug released was determined by quantification of ZnPPIX using UV-Vis spectrophotometry at 405 nm, as described above. The study was performed with three separate NE preparations, and the mean values were reported. The amount of ZnPPIX released was quantified relative to its initial concentration in the formulation.

Dissociation of GBM Tissues and Isolation of Leukocytes From Blood Samples

Following surgical excision, tumor samples were placed in MACS Tissue Storage Solution (Miltenyi Biotec) and maintained at 4°C until processing, which occurred either on the same day or within 24 h, as previously described.[4,14] To generate single-cell suspensions, samples were first rinsed with 0.9% sodium chloride to remove residual blood. Subsequently, tissue dissociation was performed using a combination of mechanical and enzymatic methods, employing the Tumor Dissociation Kit (Miltenyi Biotec) and following the manufacturer's guidelines for soft tissue specimens. Prior to surgery, peripheral blood samples were collected from GBM patients in tubes containing ethylenediaminetetraacetic acid (EDTA). Red blood cells were removed by lysis and viable peripheral blood leukocytes (PBLs) were counted using the trypan blue exclusion method.

In Vitro Model of Immunosuppressive Macrophages

Macrophages were differentiated in vitro from blood monocytes, according to a previously established protocol.[14] Peripheral blood mononuclear cells (PBMCs) were obtained from buffy coats of healthy donors (HD) through density gradient centrifugation using Ficoll-Paque PLUS (GE Healthcare, Amersham, UK). Monocytes were then isolated based on their adherence properties and seeded into 24-well culture plates. Differentiation was induced over seven days using 100 ng/mL macrophage colony-stimulating factor solution (M-CSF; Miltenyi Biotec).

NEs Uptake Studies

In vitro-derived macrophages, leukocytes from blood samples of HD, and tumor cell suspensions were incubated with ZnPPIX-loaded NEs at a final drug concentration of 5 μM for 3 h. Empty nanoemulsions (NE-Blank) were used as negative controls. Following the incubation period, samples were analyzed by flow cytometry using an LSRII instrument (BD Biosciences).

Analysis of Cellular Localization by Multispectral Imaging Flow Cytometry

An Amnis® ImageStream® imaging flow cytometer (Luminex) was used to analyze the intracellular localization of ZnPPIX, either as a free drug or encapsulated in NEs. Data analysis was analysed using IDEAS software (Luminex), with compensation matrix generated from single-stained samples. Masks within the images were generated by detecting variations in intensity within a specific channel, and were computed separately for each cell, considering its unique signal in that channel. In vitro-derived macrophages were treated with 10 μM of free ZnPPIX, NE-ZnPPIX, or NE-Blank, and incubated for 2 h at 37°C, 5% CO_2 and stained with Hoechst 33342 to evaluate ZnPPIX localization.

Evaluation of Cell Viability and CD163 Expression

In vitro-derived macrophages were treated in 24-wells plates with increasing corresponding concentrations of encapsulated or free ZnPPIX for 6 h at 37°C 5% CO_2 in order to achieve maximum efficiency in cellular internalization. Following treatment, fresh RPMI complete medium was added and the cells were incubated for 24 and 48 h. Cells were harvested and stained with LIVE/DEAD fixable Aqua (Life Technologies) and anti-CD163 APC-Cyanine7 (Biolegend) at 4°C in darkness for 20 min. To prevent nonspecific antibody binding, cells were incubated with Fc Receptor (FcR) Blocking Reagent (Miltenyi Biotec), diluted 1:25 in phosphate-buffered saline (PBS) supplemented with 1% (v/v) fetal bovine serum (FBS). Data acquisition was performed using an LSRII flow cytometer (BD Biosciences) and the results were analyzed using FlowJo software (BD Biosciences).

CellTrace Labelling and Proliferation Assay

The immunosuppressive activity of in vitro-derived macrophages, untreated or pretreated with NE-ZnPPIX, NE/Blank or free ZnPPIX, was determined by assessing the proliferation of activated CellTrace-labelled PBMCs, as previously described.[14] Briefly, allogeneic PBMC from HD were labelled with CellTrace, stimulated with 5 μg/mL anti-CD3 and 5 μg/mL soluble anti-CD28 antibodies (BioLegend) for four days and co-cultured at a 1:0.5 ratio with in vitro-derived macrophages in flat bottom 96 well plate. At the end of the culture period, the cells were harvested and stained with anti-CD3 -PE Cy7 (Beckman Coulter), and the CFSE signal of gated $CellTrace^{+}/CD3^{+}$ cells was analyzed. T cell suppression was quantified by determining the absolute number of proliferating cells using TruCount™ tubes (BD Biosciences), enabling precise cell enumeration. Proliferation levels were normalized by setting the response of T cells cultured alone as the 100% reference point.

Immune Phenotyping of the Blood and of the TME by Multiparametric Flow Cytometry Analysis

Single-cell suspensions from GBM tissues were counted and stained with LIVE/DEAD Fixable Aqua (Life Technologies, Thermo Fisher Scientific) anti-CD45 BV421 (BD Biosciences), anti-CD33 PE-Cy7 (BD Biosciences), anti-HLA-DR APC (BD Biosciences), and anti-CD49d PE (BioLegend). Blood leukocytes were stained with LIVE/DEAD Fixable Aqua (Life Technologies, Thermo Fisher Scientific) anti-CD14-FITC (BD Biosciences), anti-CD15-V450 (BD Biosciences), and anti-CD3-PE-Cy7 (Beckman Coulter). Flow cytometric acquisition was carried out using an LSRII cytometer (BD Biosciences) and data analysis was performed with FlowJo software (BD Biosciences).

Statistical Analysis

Statistical significance between two experimental groups was assessed using Student's *t*-test, while comparisons involving three or more groups were evaluated by one-way analysis of variance (ANOVA). A p-value of ≤ 0.05 was considered indicative of statistical significance. All analyses were conducted using GraphPad Prism version 8 (GraphPad Software, Dotmatics).

Results

Development and Characterization of NE-ZnPPIX

To efficiently encapsulate ZnPPIX, we selected a nanosystem in the form of an oil-in-water (O/W) NE. This choice was driven by the challenges associated with the hydrophobic nature of the compound, as oil-in-water NE provide an effective method for encapsulating and delivering ZnPPIX.

The NEs were composed of an MCT oil core stabilized by a surfactant shell composed of a mixture of hydrophilic and hydrophobic surfactants, Myrj®52 and Labrafil®M1944CS, as described by Rosso et al[17,19] After lipid assembly, ZnPPIX and EtOH were added to the mixture and the formulations were heated until complete dissolution. The solvent and the aqueous phase (PBS) were mixed using a microfluidic technique (Figure 1).

Physicochemical characterization revealed that the NEs had an average size of 109.39 ± 1.46, a PDI-value of 0.14 ± 0.02, zeta-potential values of - 10.8 ± 0.48, an encapsulation efficiency (EE) of 69.37 ± 3.54 (Table 1) and a drug loading (DL) of 0.15%. These values are in line with previous results reported for the encapsulation of hydrophobic molecules in the NE systems.[17] The average size value and zeta-potential values remain stable over time (Figure 2a). The measured concentration of the ZnPPIX loaded within the NEs was 0.14 ± 0.01 mg/mL. To determine the release profile of ZnPPIX from NE, an in vitro release rate kinetics study was performed using a dialysis bag. The release medium employed in this experiment was PBS at a pH of 6.0, chosen to mimic the typical environment found in the TME of gliomas.[20,21] The biphasic release profile of ZnPPIX from the NE is shown in Figure 2b. An initial burst release of the drug was observed, and approximately 40% of the ZnPPIX was released within 8 h. A rapid release phase was observed on the first day (Figure 2b, inset graph), during which approximately 50% of the ZnPPIX was released. This was followed by a slower phase, reaching up to 80% release within 10 days, and over 90% after 21 days. The morphological characteristics of NE-ZnPPIX were analyzed using TEM. The obtained images demonstrated that NE-ZnPPIX displayed uniform, well-defined spherical structures, with no observable differences between the blank and drug-loaded formulations. The particle sizes visualized by TEM were consistent with those obtained from DLS measurements (Figure 2c).

Uptake of NE-ZnPPIX by in Vitro-Derived Macrophages

Monocytes differentiated in vitro with M-CSF give rise to macrophages with characteristics similar to those of BMDMs, as they are immunosuppressive towards activated T cells. These cells show high expression of CD163 and PD-L1 markers, mirroring the characteristics observed in BMDMs.[4,14] As the primary goal of developing NE-ZnPPIX was to target immunosuppressive macrophages in the TME and induce their reprogramming, we used in vitro-derived macrophages as a representative model of BMDMs in our experiments. These cells offer a controlled and reproducible system for the study of macrophage-targeted drug delivery and reprogramming.

Flow cytometry and imaging studies were conducted to assess the incorporation of NE-ZnPPIX into macrophages. The natural fluorescence emission of the PPIX molecule within the encapsulated ZnPPIX was exploited for detection. Various concentrations and incubation times of NE-ZnPPIX were applied to determine the optimal conditions for cellular internalization (Figure 3). Significant time-dependent differences in uptake were observed

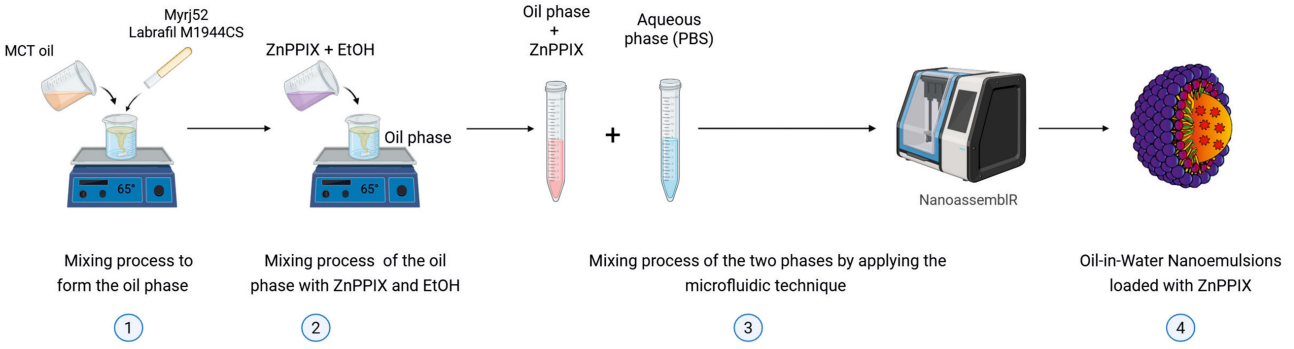

Figure 1 Schematic representation illustrating the preparation of O/W NE loaded with ZnPPIX using the microfluidic technique.

Table 1 Physicochemical Properties of NE-ZnPPIX

NE formulation	Size (nm)	PdI	ζ potential (mV)	EE%	[ZnPPIX] (mg/mL)
NE-ZnPPIX	109.39 ± 1.46	0.14 ± 0.02	− 10.8 ± 0.48	69.37 ± 3.54	0.14 ± 0.01

between the two concentrations of NE-ZnPPIX (5 μM and 10 μM) after incubation periods of 1 and 6 h, with an increase in internalization over time (Figure 3a and b). Due to space limitations in the Figure 3b, only comparisons among different time points for the same drug concentration are shown. Full details of all tests results are reported in Table S1. The cellular localization of ZnPPIX was further validated through imaging flow cytometry analysis

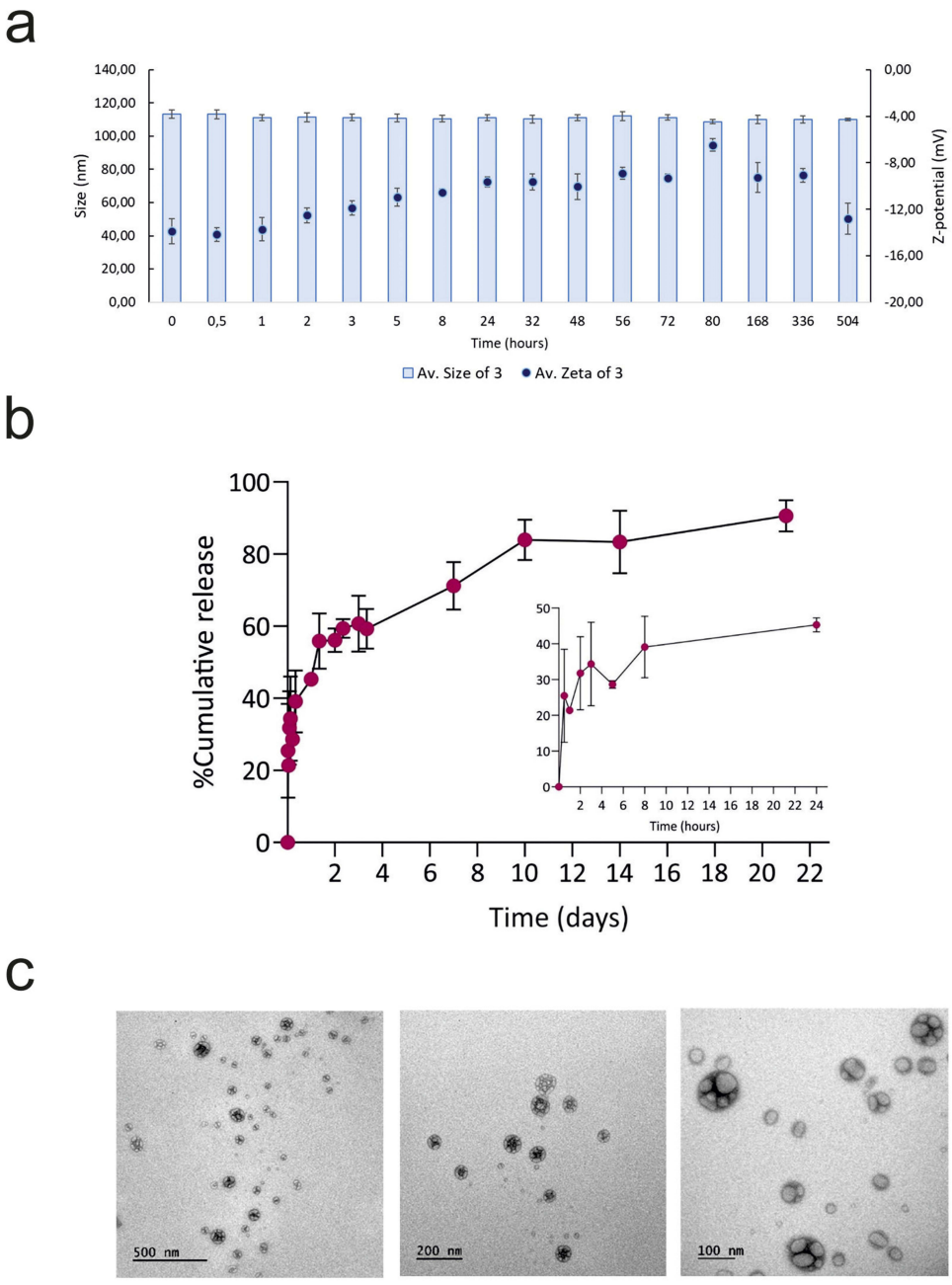

Figure 2 Development and characterization of NE-ZnPPIX. (**a**) Physicochemical property defined by DLS analysis. (**b**) Release kinetics of ZnPPIX from the NEs at pH 6. Each point shows mean ± SD (n=3). (**c**) TEM images of ZnPPIX-loaded NEs (Scale bar: 500, 200 and 100 nm).

https://doi.org/10.2147/IJN.S533321

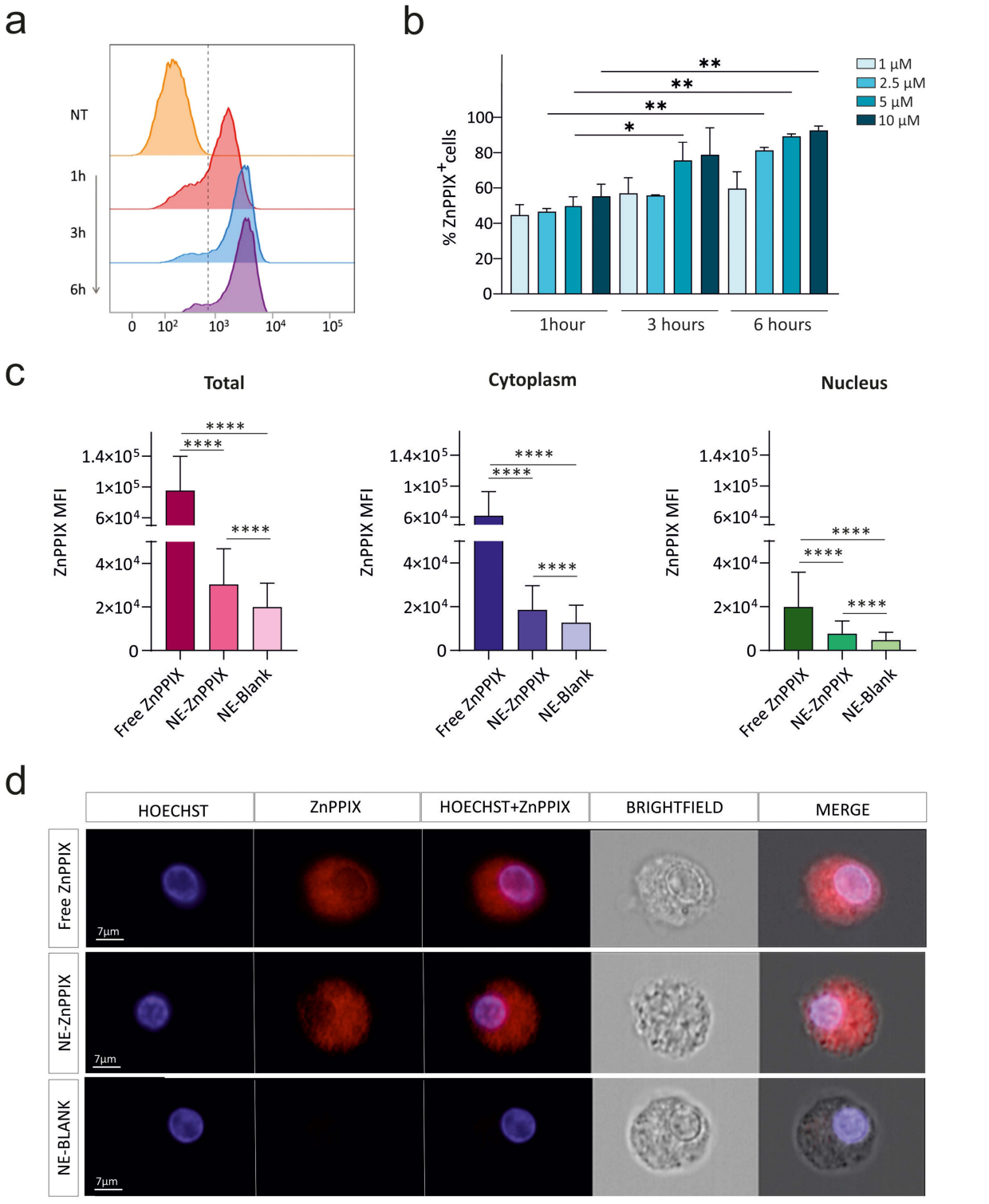

Figure 3 Cellular internalization of NE-ZnPPIX by in vitro-derived macrophages. (**a**) A representative flow cytometry analysis of untreated cells (orange) and macrophages treated with NE ZnPPIX for 1h (red), 3h (blue), 6h (violet). (**b**) Quantification in percentages of macrophages positive to ZnPPIX signal, treated with a different rage of concentration of NE-ZnPPIX and incubated at different time points, represented as mean ± SD. Comparisons were performed using a two-way ANOVA followed by Tukey's multiple comparison test (n=3). Only comparisons among different time points for the same drug concentration are shown in the graph. *$p<0.05$; **$p<0.01$ (**c**) Imaging flow cytometry analysis of ZnPPIX cellular localization. Macrophages were treated with either free ZnPPIX or NE-ZnPPIX or NE-Blank. Not treated cells were used as a negative control. Bars show the mean fluorescence intensity (MFI) ± SD of total, cytoplasmic and nuclear of ZnPPIX quantified on 1000 cells treated with the same dose of Free ZnPPIX, NE-ZnPPIX or NE-Blank. Comparisons were performed using a one-way ANOVA followed by Tukey's multiple comparisons test (n=1000). ****$p<0.0001$ (**d**) Three representative images are reported, each showing the nuclear marker Hoechst (violet), the ZnPPIX signal (red), the merged image of the two signals, the bright field (BF) and the overall merged image. Bar = 7µm.

(Figure 3c and d), a technique that allows dissection of the fluorescent signal contributions from both the cytoplasm and nucleus. As a control, macrophages treated with NE-Blank were analyzed to assess any potential impact on fluorescence. The results indicated that the incorporation of the NE-Blank did not affect the autofluorescence of the cells, whereas macrophages treated with both free and encapsulated ZnPPIX showed a distinct fluorescent signal, although a higher fluorescence intensity was observed in cells treated with free ZnPPIX. This imaging technique also permits the quantitative analysis of fluorescent signals from segmented cell areas. The data revealed that ZnPPIX was significantly localized in both the nucleus and cytoplasm of treated macrophages, showing a higher signal intensity compared to macrophages treated with NE-Blank (Figure 3c and d).

Uptake of NE-ZnPPIX by Cells Composing the GBM Microenvironment and by Blood Leukocytes

Given the promising results regarding the cellular uptake of NE-ZnPPIX by in vitro-derived macrophages, we further investigated whether this nanosystem could be incorporated by cells from freshly resected GBM specimens. To ensure biological relevance, tissue sampling was specifically directed to the non-necrotic core region of the tumor, which is rich in immunosuppressive macrophages.[4] Cell uptake was evaluated using multiparametric flow cytometry with antibodies against cell lineage markers. This approach allowed for discrimination of cellular internalization across different subsets of cells present in the TME of GBM specimens.

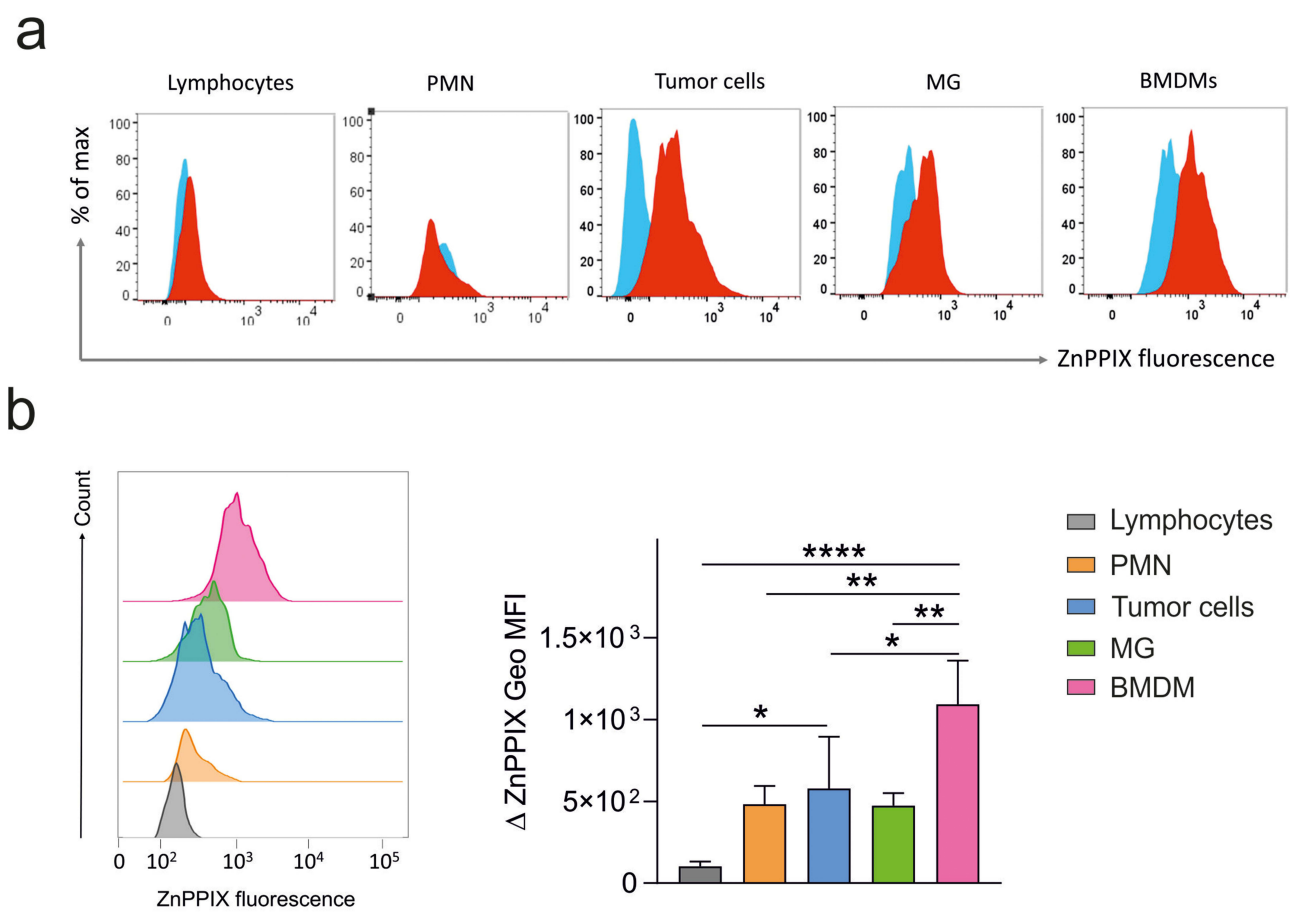

Figure 4 Uptake of NE-ZnPPIX by cells in GBM microenvironment. (**a**) A representative flow cytometry analysis showing how positive cells for ZnPPIX (red histograms) were assessed among all the cell subsets of the TME and compared to signal of NE-Blank (blue histograms) among the same populations. (**b**) Cell suspension from GBM tissue were incubated for 3h with 10μM NE-ZnPPIX or NE-Blank. MFI of ZnPPIX was calculated in BMDM (pink), MG (green), tumor cells (blue), PMN (orange), and lymphocytes (grey) (n=4). Comparisons were performed by one-way ANOVA followed by Tukey's multiple comparison test. *$p<0.05$, **$p<0.01$, ****$p<0.0001$.

https://doi.org/10.2147/IJN.S533321

The results revealed that the highest uptake of NE-ZnPPIX occurred in BMDMs, followed by tumor cells (identified as CD45^{-} cells), MG cells, and polymorphonuclear leukocytes (PMN), while lymphocytes showed negligible incorporation of NEs. As BMDMs are among the most abundant leukocytes in the GBM infiltrate and possess the highest immunosuppressive ability, these findings confirm the versatility of NE-ZnPPIX in targeting immunosuppressive cells within the TME (Figure 4).

To assess the potential of NE-ZnPPIX to target immune cells in the bloodstream, we investigated the internalization of encapsulated ZnPPIX by subsets of PBLs from HDs. Results indicate that monocytes exhibited the highest uptake capacity, followed by PMN, whereas T lymphocytes showed minimal uptake (Figure 5).

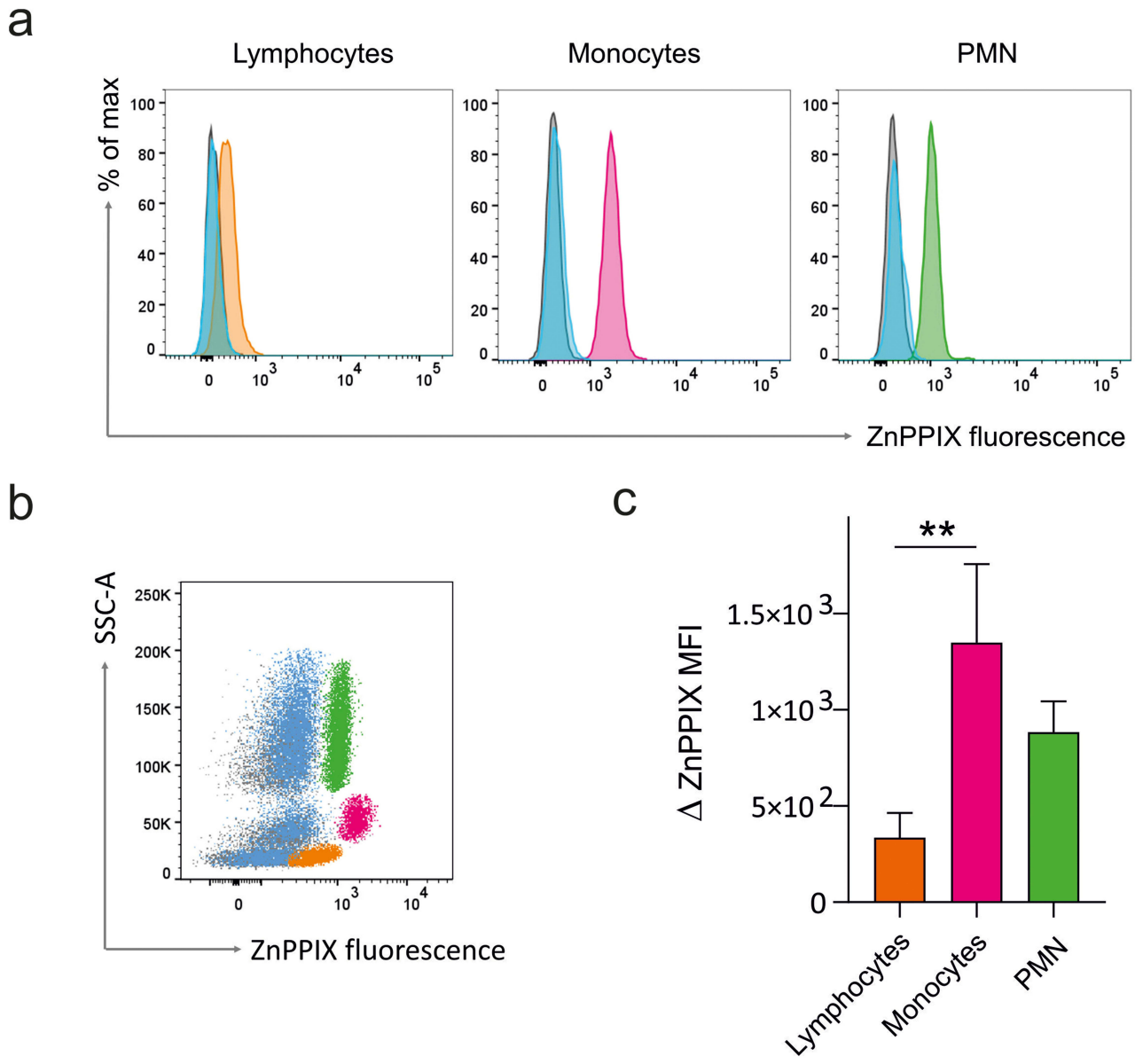

Figure 5 In vitro uptake of NE-ZnPPIX by blood leukocytes. (**a**) Leukocytes were incubated with either 10 μM NE-Blank or 10μM NE-ZnPPIX for 3 h at 37°C. Histograms show for each cell subset: untreated cells (grey), NE-Blank (light blue) and NE-ZnPPIX uptake by lymphocytes (orange), monocytes (pink) and PMN cells (green). (**b**) PBLs were incubated with NEs for 3 h and its uptake was evaluated by flow cytometry analysis. NE-ZnPPIX uptake by lymphocytes (orange), monocytes (pink), and PMN cells (green) compared with cell autofluorescence (grey) and fluorescence due to NE-Blank uptake (light blue) is shown in a representative sample. (**c**) Bars represent the mean ± SD of the ZnPPIX MFI in lymphocytes, monocytes and PMN cells (n = 3). Comparisons were performed by one-way ANOVA followed by Tukey's multiple comparison test. ***p<0.01*.

Given the uptake of NE-ZnPPIX by PMN, the major circulating leukocyte population, this finding suggested that systemic delivery may result in off-target sequestration and reduced therapeutic efficacy. In contrast, the observed internalization of these NEs by immunosuppressive myeloid populations and malignant cells within the TME highlights the potential advantages of localized administration as a more effective therapeutic strategy.

Targeting HO-1 with NE-ZnPPIX Reduces Macrophage-Mediated Immunosuppression

To evaluate the reprogramming efficiency of NE-ZnPPIX in in vitro-derived macrophages, we compared the effects of free ZnPPIX and its nanoemulsion-encapsulated form using a well-established T cell proliferation assay. Our findings indicated that the presence of both free ZnPPIX and its encapsulated form in NEs significantly restored T cell proliferation. While NE-Blank showed a tendency to improve T cell proliferation, this effect was not statistically significant (Figure 6a and b). T cell immunosuppression can also be assessed by the downregulation of CD3 expression when T cells are cultured with macrophages. Consistently, treatment of macrophages with either free ZnPPIX or NE-ZnPPIX restored CD3 expression in T cells (Figure 6b). To ensure that the effect on macrophages was not due to any cytotoxic activity of the NEs, we evaluated cell viability. We treated macrophages with increasing concentrations (1–10 μM) for up to 48 hours: no cytotoxic effects were observed upon exposure to either the empty nanoemulsion or the ZnPPIX-filled one (Figure S1).

The effects of NE-ZnPPIX on immune suppression relief were also tested in macrophages derived from a single GBM specimen following cell sorting through immunomagnetic bead-based separation, as previously described.[4,14] In this case, the results showed a recovery in the proliferation of $CD3^+$ T cells when macrophages were treated with either encapsulated ZnPPIX or the free drug, thus confirming the data obtained from the in vitro macrophage model (Figure S2).

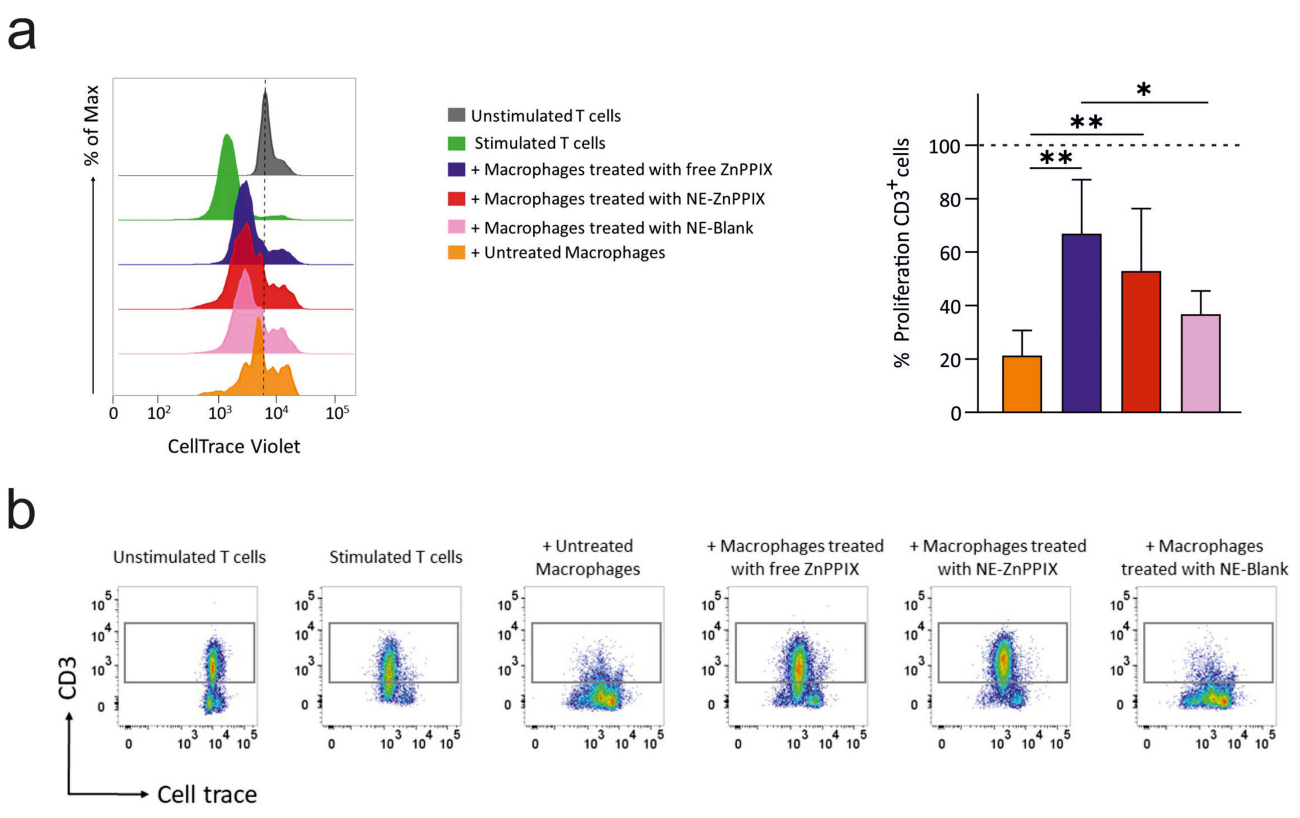

Figure 6 HO-1 inhibition in macrophages relieves immunosuppression exerted on T cells. (**a**) T cells were cultured with macrophages for 96 h (1:0.5 ratio, n=4); data were normalized assuming the proliferation of T cells alone to be 100%. The bars represent the mean ± SD. Comparisons were performed by one-way ANOVA followed by Tukey's multiple comparison test. *$p<0.05$, **$p<0.01$ (right panel). CellTrace histograms from a representative experiment of the immunosuppression assay (right panel). (**b**) Dot plots show the expression of CD3 in unstimulated T cells, stimulated T cells and T cells cultured in presence of macrophages either untreated or treated with free ZnPPIX or NEs.

https://doi.org/10.2147/IJN.S533321

NE-ZnPPIX Reduces Surface Expression of CD163 on in Vitro-Derived Macrophages

The effectiveness of HO-1 inhibition by ZnPPIX was assessed by examining its downstream effects on macrophages with a specific focus on CD163 expression. CD163 is a scavenger receptor for haptoglobin–hemoglobin complexes thus playing a critical role in heme and iron metabolism, highly expressed by BMDMs infiltrating GBM tissues. Indeed, CD163 mediates the uptake of haptoglobin–hemoglobin complexes into macrophages, where heme is subsequently degraded by HO-1 into carbon monoxide (CO), biliverdin, and iron. Both CO and biliverdin possess anti-inflammatory and antioxidant properties, contributing to a shift toward an immunosuppressive macrophage phenotype.[22] Moreover, CD163 engagement promotes IL-10 secretion, which further upregulates HO-1 expression, establishing a reinforcing anti-inflammatory loop. HO-1-derived iron also participates in immune regulation by influencing ferroportin-mediated export and intracellular iron levels, which affect macrophage polarization, redox status, and cytokine expression.[23] CD163 is extensively established as a marker of TAMs exhibiting pro-tumoral and anti-inflammatory characteristics, with its expression in both TAMs and malignant cells being associated with adverse prognoses in gliomas and other cancer types.[24]

We have previously demonstrated a significant reduction in CD163 protein expression in macrophages following HO-1 inhibition via treatment with free ZnPPIX in macrophages.[14] Based on these and other findings, CD163 expression has been proposed as a surrogate marker for macrophage immunosuppressive activity.[25] Hence, we evaluated the modulation of CD163 expression in in vitro-derived macrophages 24 h after treatment with NE-ZnPPIX and compared it to that of free ZnPPIX treatment.

Results showed that all tested concentrations of NE-ZnPPIX effectively downregulated CD163 protein expression. Interestingly, treatment with 5 μM and 10 μM NE-ZnPPIX for 24 h resulted in a greater downregulation of CD163 compared to the same concentrations of free ZnPPIX (Figure 7). These data suggest that NEs can act as depot systems capable of promoting sustained drug release and prolonging therapeutic effects.

Discussion

In recent years, various immunotherapeutic strategies have been investigated to improve outcomes in GBM, including immune checkpoint inhibitors, myeloid-targeted therapies such as CSF-1R inhibitors, and CAR T cell therapies targeting antigens like EGFR and IL13Rα2.[26–29] However, these approaches have shown limited clinical success, largely due to the highly immunosuppressive TME, characterized by regulatory T cells, myeloid-derived suppressor cells (MDSCs), and elevated expression of immune checkpoint molecules such as Programmed death ligand 1 (PD-L1). Additional barriers include tumor heterogeneity, low infiltration of effector T cells, and the presence of therapy-resistant glioma stem cells. Moreover, the altered metabolic landscape of GBM and the tumor's capacity to develop resistance mechanisms further compromise immune activation and therapeutic efficacy. Despite these challenges, numerous ongoing clinical trials are exploring innovative strategies to overcome immune evasion and improve clinical outcomes.[26,28,29] In this context, nanotechnology thus offers unique advantages that may address several challenges associated with the conventional treatment approaches for GBM.[30–32]

An additional and significant limitation in GBM therapy is posed by the blood–brain barrier (BBB), a tightly regulated interface that restricts the entry of most therapeutic agents into the central nervous system (CNS). Although the BBB is locally disrupted in GBM, this disruption is heterogeneous, leading to uneven drug distribution and subtherapeutic concentrations in parts of the tumor. To overcome this problem, nanomedicine has emerged as a promising strategy: various engineered nanocarriers, such as liposomes, polymeric nanoparticles, dendrimers, micelles, and carbon- or metal-based materials, have been developed to enhance BBB penetration through receptor-mediated transcytosis or passive diffusion, while offering tumor specificity, controlled release, and immunomodulatory potential.[33] Additionally, more advanced delivery systems can potentially be optimized through the integration of artificial intelligence into their design.[34,35] In this study, we propose a novel nanomedicine designed to normalize the immunosuppressed TME and enhance the anti-tumor activity of the immune system.

We decided to exploit the immunomodulatory properties of ZnPPIX, a first-generation HO-1 inhibitor, which targets an enzyme implicated in heme catabolism and overexpressed in various cancers, including GBM. In the tumoral context, HO-1 participates in tumor cell proliferation, angiogenesis, and metastasis progression by sustaining iron metabolism in

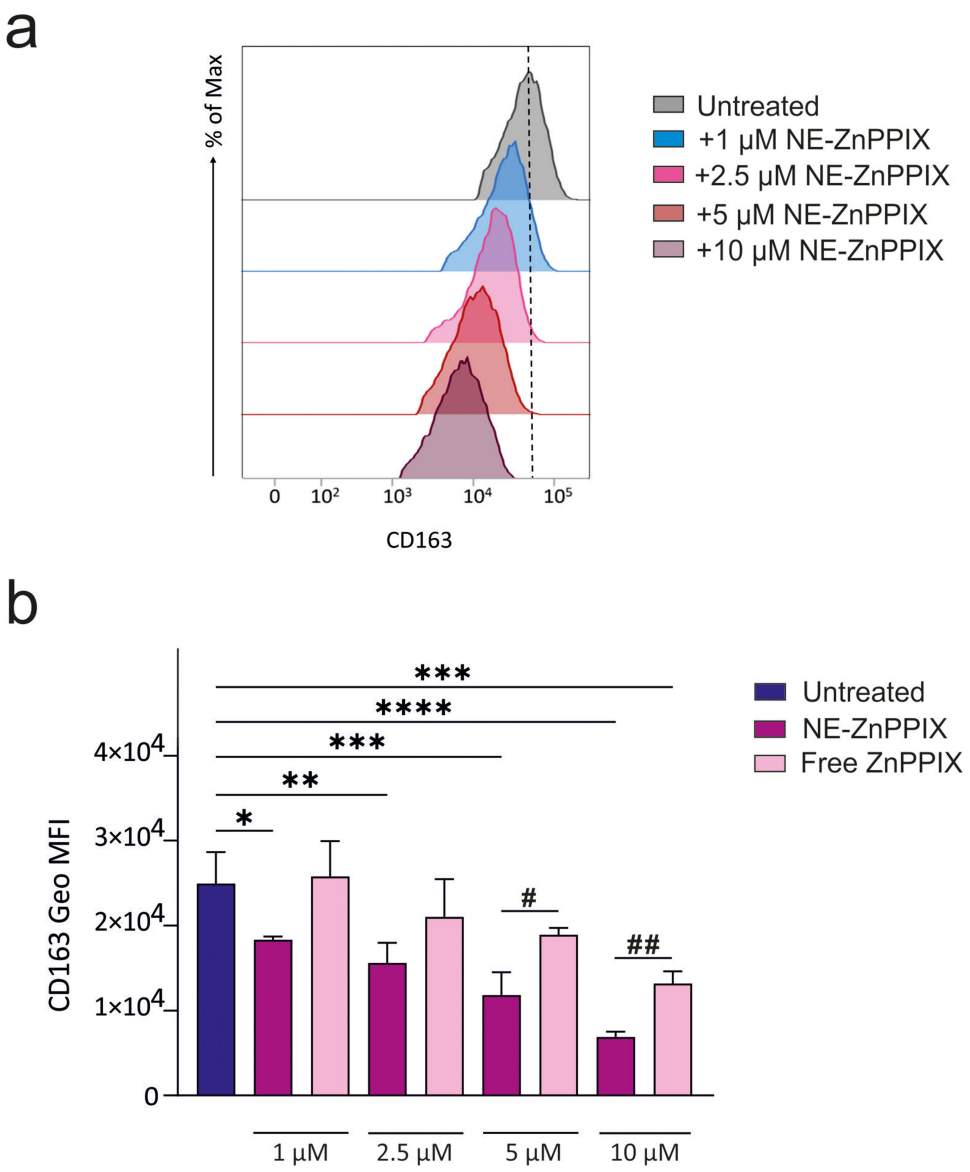

Figure 7 Evaluation of CD163 expression on in-vitro derived macrophages after 24 h of treatment. (**a**) A representative example of flow cytometry analysis of the modulation of CD163 expression. (**b**) Macrophages were treatment with different concentrations of NE ZnPPIX (purple bars) and free drug (pink bars). All comparisons among treated cells were performed versus untreated cells through one-way ANOVA followed by Tukey's multiple comparison test. *$p<0.05$; **$p<0.01$; ***$p<0.001$; ****$p<0.0001$. Comparison between NE-ZnPPIX and free ZnPPIX for the same concentration were performed by using Student's *t*-test. $^{\#}p<0.05$, $^{\#\#}p<0.01$ (n=3).

rapidly growing cells. Our findings support the notion that inhibition of HO-1 disrupts the immune suppression function exerted by BMDMs and in vitro derived macrophages, consistent with our previous work. Moreover, ZnPPIX was identified as the most effective inhibitor, among other metalloporphyrins structurally similar to heme, that can compete with it for binding to HO-1 enzyme and therefore induce modulation of BMDMs' activity.[14]

Characterization studies of an O/W NE containing ZnPPIX demonstrated that it presented a stabilized structure with a size of 109±1.46 nm, a slightly negative zeta potential of −10.8±0.48 mV, an encapsulation efficiency (EE) of 69.37±3.54% (Table 1) and drug loading (DL) of 0.15. Of note, the small particle size of NE-ZnPPIX may facilitate its crossing of the disrupted BBB in GBM, potentially allowing it to reach the TME. However, further studies are needed to test the ability to cross the BBB in order to achieve therapeutic efficacy and safety of these NEs. To address the heterogeneity and limitations of BBB permeability, a local administration strategy could be envisaged to ensure targeted delivery to the tumor site. To further evaluate the therapeutic potential of NE-ZnPPIX, incorporation studies using in vitro-derived model of macrophages, as well as primary cells from GBM specimens and blood samples

https://doi.org/10.2147/IJN.S533321

confirmed the capacity of these NE-ZnPPIX to be efficiently internalized by immunosuppressive macrophages and circulating monocytes (Figures 3–5). Moreover, our results showed that targeting HO-1 with NE-ZnPPIX significantly reduced the immunosuppressive activity of these cells (Figure 6 and Figure S2), in line with our previous findings.[14] In addition, NE-ZnPPIX showed superior efficacy in modulating macrophage activity and reducing the expression of CD163, a marker associated with the pro-tumoral and immunosuppressive phenotypes, compared to free ZnPPIX treatment (Figure 7).

Internalization studies (Figure 5) revealed substantial incorporation by PMN, which constitute 50–70% of circulating leukocytes. Consequently, systemic administration could lead to significant off-target accumulation and potential hematological effects. Therefore, we believe that local administration strategies would minimize systemic exposure while maintaining therapeutic concentrations at the tumor site. This strategy may include intraoperative application or convection-enhanced delivery, both of which are feasible in the context of GBM's localized nature. The adoption of local administration approaches would offer distinct advantages in terms of both clinical relevance and biological rationale. First of all, it would bypass the need for systemic BBB penetration. Moreover, by targeting the surgical cavity, our nanoemulsion could directly target tumor-associated immunosuppressive macrophages. This aligns with existing clinical approaches for local therapy (eg, Gliadel wafers)[36] and leverages the compromised BBB at the resection margins to enhance drug retention and uptake.

ZnPPIX, a first-generation HO-1 inhibitor, targets an enzyme implicated in heme catabolism and is overexpressed in various cancers including GBM. In the tumoral context, HO-1 participates in tumor cell proliferation, angiogenesis, and metastasis progression by sustaining iron metabolism in rapidly growing cells. Our findings support the notion that inhibition of HO-1 disrupts the immune suppression function exerted by BMDMs and in vitro-derived macrophages, consistent with our previous work.[14] Moreover, ZnPPIX was identified as the most effective inhibitor among other metalloporphyrins structurally similar to heme that can compete with it for binding to HO-1 enzyme and therefore induce modulation of BMDMs' activity. While our results align with other studies exploring immune checkpoint inhibitors and myeloid modulation,[37,38] our approach is distinct in employing a ZnPPIX-loaded NE specifically used with the final aim of targeting BMDMs within the GBM microenvironment. Other nanoparticle-based systems have utilized Toll-Like receptor (TLR) agonists or Signal transducer and activator of transcription 3 (STAT3) inhibitors to reprogram macrophages;[39,40] our findings complement these efforts and offer the additional advantage of selective delivery and intrinsic ZnPPIX fluorescence, which enables real-time monitoring of cellular uptake.

While our data demonstrate that nanoencapsulation prolongs ZnPPIX release and maintains its bioactivity, we acknowledge that comprehensive pharmacokinetic studies are needed to fully characterize the delivery advantages of NE-ZnPPIX. In vivo studies are essential for translational research, as they provide critical insights into biodistribution, circulation time, and tumor accumulation. Although this proof-of-concept study was conducted in vitro, it establishes a strong foundation for future investigations aimed at confirming the therapeutic potential and delivery efficiency of this nanoformulation in relevant GBM models.

Conclusions

Drug-loaded nanosystems offer significant potential for the advancement of targeted and personalized treatments for GBM and other cancers. In this study, rather than utilizing conventional drugs, we propose a novel agent, ZnPPIX, encapsulated in a NE to normalize the immunosuppressive TME. ZnPPIX is a potent inhibitor of HO-1, a key enzyme in iron metabolism and the immunosuppressive activity of TAMs.

Our findings suggest that NE-ZnPPIX has the potential to remodel the TME, thereby offering an innovative strategy for enhancing the immune response against GBM.

Additionally, our nanoformulation demonstrated excellent biocompatibility with target cells (macrophages) showing a viability higher than 90% for the tested concentrations. To further optimize therapeutic outcomes, future approaches should integrate nanotechnology with immunostimulatory therapies, such as immune checkpoint inhibitors (eg, anti-programmed death-1 (anti-PD-1) and anti-cytotoxic T lymohocyte-associated antigen 4 (anti-CTLA-4)). Such combination could enhance the targeted delivery and efficacy of immunomodulatory agents, overcoming the challenges of immune evasion and improving the overall anti-tumor immune response in GBM.

Abbreviations

heme oxygenase-1, HO-1; NE, nanoemulsions; ZnPPIX, Zinc protoporphyrin IX; TME, tumor microenvironment; GBM, glioblastoma multiforme; HD, healthy donor; PBMC, peripheral blood mononuclear cell; BMDM, bone marrow-derived macrophages; MG, microglia; PMN, polymorphonuclear cell; MFI, mean fluorescence intensity.

Data Sharing Statement

All data generated or analysed during this study are included in this published article and will be available from the corresponding author upon reasonable request.

Ethics Approval and Consent to Participate

The ethical committees of IOV-IRCCS, Padua University Hospital, and Florence University Hospital approved all experiments, and all patients gave their informed consent. This study was conducted in full compliance with the ethical principles of the Declaration of Helsinki.

Acknowledgments

We would like to thank Norma Muraro and Beatrice Musca for helpful discussions and Dr. Mattia Albiero and Dr. Loris Bertazza for their support with the imaging flow cytometry analysis.

Author Contributions

All authors made a significant contribution to the work reported, whether that is in the conception, study design, execution, acquisition of data, analysis and interpretation, or in all these areas; took part in drafting, revising or critically reviewing the article; gave final approval of the version to be published; have agreed on the journal to which the article has been submitted; and agree to be accountable for all aspects of the work.

Funding

This work was supported by Università degli Studi di Padova (SID 2020, DiSCOG), Ministero della Salute (RF-2019-12369251), Intramural Research Funding Programs IOV-IRCCS 5×1000 Cancerplat-2 BIOV19MANDR to SM, by the Italian Ministry of Health "Ricerca Corrente" and the ARQUS project (ANR) 2023-2025 to GL.

Disclosure

The authors declare that they have no competing interests in this work.

References

1. Barry ST, Gabrilovich DI, Sansom OJ, Campbell AD, Morton JP. Therapeutic targeting of tumour myeloid cells. *Nat Rev Cancer*. 2023;23(4):216–237. doi:10.1038/s41568-022-00546-2
2. Sampson JH, Gunn MD, Fecci PE, Ashley DM. Brain immunology and immunotherapy in brain tumours. *Nat Rev Cancer*. 2020;20(1):12–25. doi:10.1038/s41568-019-0224-7
3. Zou Y, Wang YB, Xu S, et al. Brain co-delivery of temozolomide and cisplatin for combinatorial glioblastoma chemotherapy. *Adv Mater*. 2022;34(33). doi:10.1002/adma.202203958.
4. Pinton L, Masetto E, Vettore M, et al. The immune suppressive microenvironment of human gliomas depends on the accumulation of bone marrow-derived macrophages in the center of the lesion. *J Immunother Cancer*. 2019;7(1):7. doi:10.1186/s40425-018-0467-y
5. Kowal J, Kornete M, Joyce JA. Re-education of macrophages as a therapeutic strategy in cancer. *Immunotherapy*. 2019;11(8):677–689. doi:10.2217/imt-2018-0156
6. Klemm F, Maas RR, Bowman RL, et al. Interrogation of the microenvironmental landscape in brain tumors reveals disease-specific alterations of immune cells. *Cell*. 2020;181(7):1643–+. doi:10.1016/j.cell.2020.05.007
7. Liu Y, Zhou F, Ali H, Lathia JD, Chen PW. Immunotherapy for glioblastoma: current state, challenges, and future perspectives. *Cell Mol Immunol*. 2024;21(12):1354–1375. doi:10.1038/s41423-024-01226-x
8. Olivet MM, Brown MC, Reitman ZJ, et al. Clinical applications of immunotherapy for recurrent glioblastoma in adults. *Cancers*. 2023;15(15):3901. doi:10.3390/cancers15153901
9. Fu WL, Wang WJ, Li H, et al. Single-cell atlas reveals complexity of the immunosuppressive microenvironment of initial and recurrent glioblastoma. *Front Immunol*. 2020;11:11. doi:10.3389/fimmu.2020.00011

10. Magri S, Musca B, Bonaudo C, et al. Sustained accumulation of blood-derived macrophages in the immune microenvironment of patients with recurrent glioblastoma after therapy. *Cancers*. 2021;13(24):6178. doi:10.3390/cancers13246178
11. Mohme M, Schliffke S, Maire CL, et al. Immunophenotyping of newly diagnosed and recurrent glioblastoma defines distinct immune exhaustion profiles in peripheral and tumor-infiltrating lymphocytes. *Clin Cancer Res*. 2018;24(17):4187–4200. doi:10.1158/1078-0432.CCR-17-2617
12. Li JA, Yang J, Jiang SP, et al. Targeted reprogramming of tumor-associated macrophages for overcoming glioblastoma resistance to chemotherapy and immunotherapy. *Biomaterials*. 2024;311.
13. Perrin SL, Samuel MS, Koszyca B, et al. Glioblastoma heterogeneity and the tumour microenvironment: implications for preclinical research and development of new treatments. *Biochem Soc Trans*. 2019;47(2):625–638. doi:10.1042/BST20180444
14. Magri S, Musca B, Pinton L, et al. The immunosuppression pathway of tumor-associated macrophages is controlled by heme oxygenase-1 in glioblastoma patients. *Int J Cancer*. 2022;151(12):2265–2277. doi:10.1002/ijc.34270
15. Farokhzad OC, Langer R. Impact of nanotechnology on drug delivery. *Acs Nano*. 2009;3(1):16–20. doi:10.1021/nn900002m
16. Mitchell MJ, Billingsley MM, Haley RM, Wechsler ME, Peppas NA, Langer R. Engineering precision nanoparticles for drug delivery. *Nat Rev Drug Discov*. 2021;20(2):101–124. doi:10.1038/s41573-020-0090-8
17. Andretto V, Taurino G, Guerriero G, et al. Nanoemulsions embedded in alginate beads as bioadhesive nanocomposites for intestinal delivery of the anti-inflammatory drug tofacitinib. *Biomacromolecules*. 2023;24(6):2892–2907. doi:10.1021/acs.biomac.3c00260
18. Rosso A, Andretto V, Chevalier Y, et al. Nanocomposite sponges for enhancing intestinal residence time following oral administration. *J Control Release*. 2021;333:579–592. doi:10.1016/j.jconrel.2021.04.004
19. Rosso A, Lollo G, Chevalier Y, et al. Development and structural characterization of a novel nanoemulsion for oral drug delivery. *Colloid Surf A*. 2020;593.
20. Boyd NH, Tran AN, Bernstock JD, et al. Glioma stem cells and their roles within the hypoxic tumor microenvironment. *Theranostics*. 2021;11 (2):665–683. doi:10.7150/thno.41692
21. Walsh JJ, Parent M, Akif A, et al. Imaging hallmarks of the tumor microenvironment in glioblastoma progression. *Front Oncol*. 2021;11.
22. Vijayan V, Wagener FADTG, Immenschuh S. The macrophage heme-heme oxygenase-1 system and its role in inflammation. *Biochem Pharmacol*. 2018;153:159–167. doi:10.1016/j.bcp.2018.02.010
23. Yang H, Wang HC, Wang YJ, et al. Identification of CD163 as an anti-inflammatory receptor for HMGB1-haptoglobin complexes. *J Immunol*. 2016;196(1_Supplement):189.17. doi:10.4049/jimmunol.196.Supp.189.17
24. Skytthe MK, Graversen JH, Moestrup SK. Targeting of CD163 macrophages in inflammatory and malignant diseases. *Int J Mol Sci*. 2020;21(15). doi:10.3390/ijms21155497
25. Liu SS, Zhang CQ, Maimela NR, et al. Molecular and clinical characterization of CD163 expression via large-scale analysis in glioma. *Oncoimmunology*. 2019;8(7):e1601478. doi:10.1080/2162402X.2019.1601478
26. Bagley SJ, Kothari S, Rahman R, et al. Glioblastoma clinical trials: current landscape and opportunities for improvement. *Clin Cancer Res*. 2022;28 (4):594–602. doi:10.1158/1078-0432.CCR-21-2750
27. Bagley SJ, Logun M, Fraietta JA, et al. Intrathecal bivalent CAR T cells targeting EGFR and IL13Rα2 in recurrent glioblastoma: Phase 1 trial interim results. *Nat Med*. 2024;30(5):1320–1329. doi:10.1038/s41591-024-02893-z
28. Singh K, Batich KA, Wen PY, et al. Designing clinical trials for combination immunotherapy: a framework for glioblastoma. *Clin Cancer Res*. 2022;28(4):585–593. doi:10.1158/1078-0432.CCR-21-2681
29. Yu MW, Quail DF. Immunotherapy for glioblastoma: current progress and Challenge. *Front Immunol*. 2021;12.
30. Boone CE, Wang L, Gautam A, Newton IG, Steinmetz NF. Combining nanomedicine and immune checkpoint therapy for cancer immunotherapy. *Wires Nanomed Nanobi*. 2022;14(1). doi:10.1002/wnan.1739
31. Irvine DJ, Dane EL. Enhancing cancer immunotherapy with nanomedicine. *Nat Rev Immunol*. 2020;20(5):321–334. doi:10.1038/s41577-019-0269-6
32. Martin JD, Cabral H, Stylianopoulos T, Jain RK. Improving cancer immunotherapy using nanomedicines: progress, opportunities and challenges. *Nat Rev Clin Oncol*. 2020;17(4):251–266. doi:10.1038/s41571-019-0308-z
33. Grover A, Hirani A, Pathak Y, Sutariya V. Brain-targeted delivery of docetaxel by glutathione-coated nanoparticles for brain cancer. *AAPS Pharm Sci Tech*. 2014;15(6):1562–1568. doi:10.1208/s12249-014-0165-0
34. Achar A, Myers R, Ghosh C. Drug delivery challenges in brain disorders across the blood-brain barrier: novel methods and future considerations for improved therapy. *Biomedicines*. 2021;9(12):1834. doi:10.3390/biomedicines9121834
35. Habeeb M, Vengateswaran HT, You HW, Saddhono K, Aher KB, Bhavar GB. Nanomedicine facilitated cell signaling blockade: difficulties and strategies to overcome glioblastoma. *J Mater Chem B*. 2024;12(7):1677–1705. doi:10.1039/D3TB02485G
36. Shibahara I, Miyasaka K, Sekiguchi A, et al. Long-term follow-up after BCNU wafer implantation in patients with newly diagnosed glioblastoma. *J Clin Neurosci*. 2021;86:202–210. doi:10.1016/j.jocn.2021.01.037
37. Habashy KJ, Mansour R, Moussalem C, Sawaya R, Massaad MJ. Challenges in glioblastoma immunotherapy: mechanisms of resistance and therapeutic approaches to overcome them. *Br J Cancer*. 2022;127(6):976–987. doi:10.1038/s41416-022-01864-w
38. Reardon DA, Brandes AA, Omuro A, et al. Effect of nivolumab vs bevacizumab in patients with recurrent glioblastoma the checkmate 143 phase 3 randomized clinical trial. *JAMA Oncol*. 2020;6(7):1003–1010. doi:10.1001/jamaoncol.2020.1024
39. Roque D, Cruz N, Ferreira HA, et al. Nanoparticle-based treatment in glioblastoma. *J Pers Med*. 2023;13(9):1328. doi:10.3390/jpm13091328
40. Ma J, Chen CC, Li M. Macrophages/microglia in the glioblastoma tumor microenvironment. *Int J Mol Sci*. 2021;22(11).